How to cite: *Angew. Chem. Int. Ed.* **2021**, *60*, 16480–16486
International Edition: doi.org/10.1002/anie.202103170
German Edition: doi.org/10.1002/ange.202103170

VIP **Cobalt Complexes** **Very Important Paper**

A Pair of Cobalt(III/IV) Terminal Imido Complexes

Weiqing Mao, Dominik Fehn, Frank W. Heinemann, Andreas Scheurer, Dominik Munz, and Karsten Meyer**

Abstract: *The reaction of the cobalt(I) complex [(TIMMN^{mes})Co^{I}](BPh$_4$) (**2**) (TIMMN^{mes} = **t**ris-[2-(3-mesityl-**im**idazolin-2-ylidene)**m**ethyl]ami**n**e) with 1-adamantylazide yields the cobalt(III) imido complex [(TIMMN^{mes})Co^{III}(NAd)](BPh$_4$) (**3**) with concomitant release of dinitrogen. The N-anchor in diamagnetic **3** features an unusual, planar tertiary amine, which results from repulsive electrostatic interaction with the filled d(z^2)-orbital of the cobalt ion and negative hyperconjugation with the neighboring methylene groups. One-electron oxidation of **3** with [FeCp$_2$](OTf) provides access to the rare, high-valent cobalt(IV) imido complex [(TIMMN^{mes})Co^{IV}(NAd)](OTf)$_2$ (**4**). Despite a half-life of less than 1 h at room temperature, **4** could be isolated at low temperatures in analytically pure form. Single-crystal X-ray diffractometry and EPR spectroscopy corroborate the molecular structure and the d^5 low-spin, S = 1/2, electron configuration. A computational analysis of **4** suggests high covalency within the Co^{IV}=NAd bond with non-negligible spin density located at the imido moiety, which translates into substantial triplet nitrene character.*

Introduction

Terminal imido complexes of the late-transition metals are attracting increasing attention as they are often implicated as key intermediates in metal-catalyzed nitrogen-group transfers to alkenes (aziridination) and C–H bonds (amination).[1] Hence, metal imido complexes are appealing synthetic targets. This is particularly relevant for complexes of the earth-abundant 3d metals, which may give rise to various electronic structures of the imido ligand. These formal imides have been described as a) "classic" closed-shell double- or triple-bonded, dianionic RN^{2-} ligands, b) "imidyl" ligands with one unpaired electron residing at the imido ligand, or c) a metal-coordinating singlet[2] or triplet[3] "nitrene" with a formal electron sextet at the nitrogen atom. It is important to note that the accumulation of spin density at the imido ligand is thought to be essential for its high reactivity with, for example, C–H bonds.[4] In general, the reactivity of late transition metal terminal imido complexes is controlled by the formal oxidation and spin state of the metal ion as well as the coordination number. Late transition metal imido complexes in high oxidation states are rare, which is somewhat surprising, given that electron-rich imido ligands are excellent candidates for the stabilization of an electron-deficient metal ion. So far, several high-valent, formal iron(IV),[5] iron(V),[6] and iron(VI)[7] imido species have been reported. Considerably fewer high-valent metal imido complexes of cobalt,[8] nickel,[9] and copper have been reported.[2,3,10] For example, the known cobalt imido complexes span a series of oxidation states, ranging from cobalt(II) to cobalt(V).[8,11,12] Among them, low- to mid-valent cobalt(II)[11] and cobalt(III)[12] imido complexes have been the subject of intensive studies. In contrast, few investigations on high-valent cobalt imido species have been published. To the best of our knowledge, Deng's bisimido cobalt(IV) and cobalt(V) complexes [(IMes)Co(NDipp)$_2$][8] and [(IMes)Co(NDipp)$_2$](BAr$^F_4$), stabilized by an ancillary N-heterocyclic carbene (NHC) ligand, are the only examples of structurally characterized cobalt(IV) and cobalt(V) imido complexes. A monoimido cobalt(IV) complex has remained elusive.

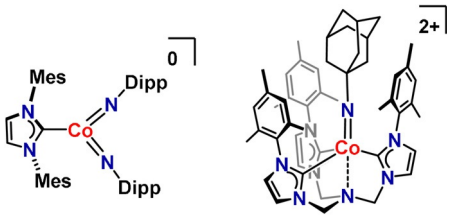

Deng, 2014 ***this work***

The aforementioned situation prompted us to explore high-valent cobalt imido complexes supported by a new, recently developed, tripodal N-heterocyclic carbene (NHC) ligand, which prevents the formation of bisimido complexes. Herein, we report an unprecedented pair of Co^{III}/Co^{IV} monoimido complexes, with a rare case of an sp^2-hybridized, tertiary amine in the Co^{III} imido complex, and the first

[*] Dr. W. Mao, D. Fehn, Dr. F. W. Heinemann, Dr. A. Scheurer, Prof. Dr. D. Munz, Prof. Dr. K. Meyer
Friedrich-Alexander-Universität Erlangen-Nürnberg (FAU)
Inorganic Chemistry
Egerlandstrasse 1, 91058 Erlangen (Germany)
E-mail: karsten.meyer@fau.de
Prof. Dr. D. Munz
Current address: Saarland University
Inorganic Chemistry: Coordination Chemistry
Campus C4.1, 66123 Saarbrücken (Germany)
E-mail: dominik.munz@uni-saarland.de

Supporting information and the ORCID identification numbers for the authors of this article can be found under: https://doi.org/10.1002/anie.202103170.

example of a fully characterized cobalt(IV) monoimido complex, including its solid-state molecular structure.

Results and Discussion

Starting from the purple cobalt(II) complex [(TIMMN^{mes})Co^{II}(Cl)](PF$_6$) (**1**; Scheme 1), obtained from the one-pot reaction of $CoCl_2$ with [H$_3$TIMMN^{mes}](PF$_6$)$_3$[13] and three equivalents of LiHMDS (71% yield), the corresponding cobalt(I) complex **2** was accessible. Reduction of a suspension of divalent **1** in tetrahydrofuran with sodium amalgam in the presence of sodium tetraphenylborate ($NaBPh_4$) led, after workup, to a green powder of the cobalt(I) complex [(TIMMN^{mes})Co^{I}](BPh$_4$) (**2**; 64% yield; Scheme 1). Complexes **1** and **2** were characterized by single-crystal X-ray diffraction (SC-XRD) analyses (Figure 1) as well as UV/Vis electronic absorption and IR vibrational spectroscopy (Figures S2 and S3, and Figures S8 and S9, respectively), SQUID magnetometry (Figure S6 and Figure S10), and CHN elemental analysis. In the molecular structure of divalent **1**, the cobalt metal ion adopts a distorted trigonal bipyramidal geometry with the three carbene entities forming the plane and the N-anchor and the chlorido ligand occupying the axial positions (Co: $d_{oop} = 0.643(2)$ Å out of the plane defined by the three carbene carbon atoms). Compared to the literature-known and closely related Co^{II} chloride TIMEN derivative [(TIMEN^{xyl})Co^{II}Cl]$^+$,[14] the nitrogen anchor atom in **1** is closer to the divalent cobalt ion, as evident by a Co–N1 distance of 2.590(3) Å compared to Co–N1 = 3.061 Å in [(TIMEN^{xyl})Co^{II}Cl]$^+$. DFT calculations revealed (Figure S33) that there is considerable orbital overlap between the d-orbitals of the cobalt ion and the p-orbitals of the N(anchor) atom in **1**, but the bond order is merely 0.14. Hence, the Co–N1 interaction is weak. Variable-temperature and variable-field (VT-VF) SQUID measurements of a microcrystalline sample of **1** revealed a magnetic moment (μ_{eff}) of 4.28 μ_B at room temperature, thus supporting the high-spin $S = 3/2$, Co^{II}, d^7 electronic structure assignment (Figure S6). Thus, the room-temperature moment of **1** falls within the range of 4.3 μ_B to 4.8 μ_B, which is typically observed for high-spin cobalt(II) complexes with pseudotetrahedral or lower symmetry,[15] and is suggestive of a quartet spin ground state for the Co^{II} complex **1**. Upon reduction, the axially bound chlorido ligand in **1** is removed, the N-anchor binds the cobalt ion (d(Co–N1) = 2.245(2) Å), and, consequently, pulls it deeper into the electron-rich cavity of TIMMN^{mes}. However, the cobalt atom in monovalent **2** is still located a remarkable 0.3306(7) Å above the plane of the three carbene moieties (d_{oop}; Scheme 1 and Figure 1).

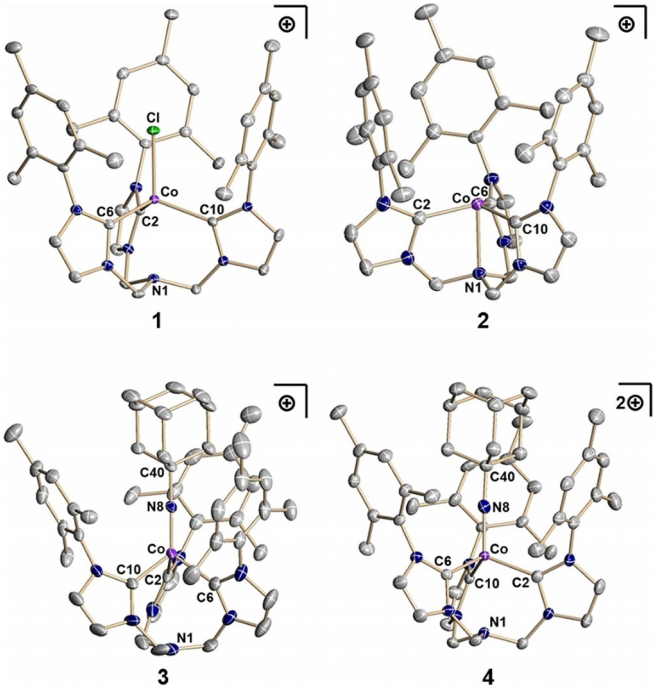

Figure 1. Molecular structures of the complex cations [(TIMMN^{mes})Co^{II}Cl]$^+$ (**1**)$^+$ in crystals of [(TIMMN^{mes})Co^{II}Cl](PF$_6$)·2 CH$_3$CN, [(TIMMN^{mes})Co^{I}]$^+$ (**2**)$^+$ in crystals of [(TIMMN^{mes})Co^{I}](BPh$_4$)·0.5 C$_7$H$_8$, [(TIMMN^{mes})Co^{III}(NAd)]$^+$ (**3**)$^+$ in crystals of [(TIMMN^{mes})Co^{III}(NAd)](BPh$_4$)·2 C$_6$H$_6$, and [(TIMMN^{mes})Co^{IV}(NAd)]$^{2+}$ (**4**)$^{2+}$ in crystals of [(TIMMN^{mes})Co^{IV}(NAd)](OTf)$_2$·2.5 C$_4$H$_{10}$O; hydrogen atoms and solvent molecules are omitted for clarity. Thermal ellipsoids are displayed at 50% probability. For CCDC depository numbers, see the Supporting Information.

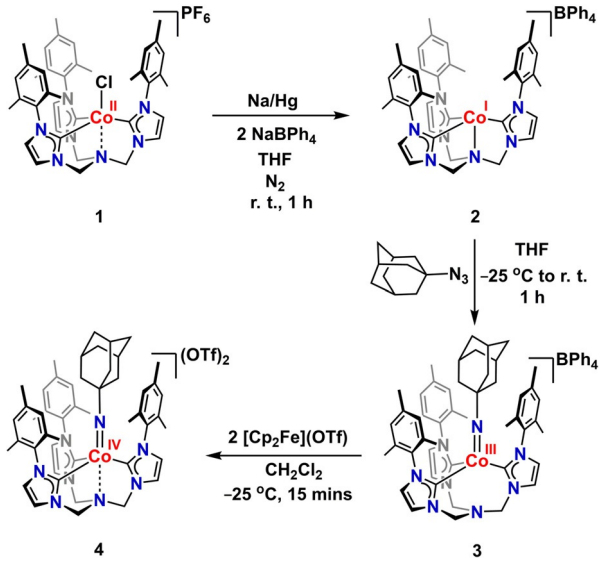

Scheme 1. Synthesis of target complexes [(TIMMN^{mes})Co^{III}(NAd)](BPh$_4$) (**3**) and [(TIMMN^{mes})Co^{IV}(NAd)](OTf)$_2$ (**4**). TIMMN^{mes} = **t**ris-[2-(3-mesityl**im**idazolin-2-ylidene)**m**ethyl]ami**n**e, Ad = adamantyl.

The reaction of monovalent **2** with one equivalent of 1-adamantyl azide (Ad-N$_3$) provides the violet cobalt(III) imido complex [(TIMMN^{mes})Co^{III}(NAd)](BPh$_4$) (**3**) in 87% yield (Scheme 1). Complex **3** is diamagnetic (d^6 low-spin, $S = 0$), and the ^{1}H and ^{13}C NMR spectra reveal C_3 symmetry in solution. The characteristic ^{1}H NMR signals for the protons of the adamantyl group were observed at 1.20, 1.10, 1.04, 0.28, and −0.85 ppm. Single-crystal X-ray diffraction analysis (SC-XRD) of crystals of trivalent **3**, obtained by the slow evaporation of a THF/benzene mixture at room temperature, revealed a four-coordinate complex cation with a well-

separated BPh_4^- counter anion (Figure 1). In the molecular structure of **3**, the TIMMN^{mes} ligand coordinates in a tridentate fashion, and the amine anchor does not show a considerable interaction with the cobalt ion (d(Co–N1) = 3.374(2) Å). This results in a pseudotetrahedral coordination environment, as further illustrated by the 0.964(1) Å offset of the metal center above the trigonal plane defined by the three NHC ligands. The Co–N(imido) bond (d(Co–N8) = 1.649(1) Å) is within the range of previously reported cobalt(III) imido complexes (1.61–1.71 Å).[12]

The N(imido)–C(adamantyl) bond of 1.438(2) Å is slightly shorter than those of typical N–C single bonds (1.45 Å). This situation is also observed in other structurally characterized cobalt(III) adamantyl imido complexes, such as [(Me_2NN)Co(NAd)] (1.435(5) Å; Me_2NN = (2,6-$C_6H_3Me_2$)NC(Me)CHC(Me)N(2,6-$C_6H_3Me_2$)$^-$),[12c] [Tp^{tBu,Me}Co(NAd)] (1.441(3) Å; Tp^{tBu,Me} = hydro-tris(3-^{t}Bu,5-Me-pyrazolyl)borate),[12e] [(giso)Co(NAd)] (1.434(5) Å; giso$^-$ = (ArN)$_2$CN(C_6H_{11})$_2^-$, Ar = 2,6-diisopropylphenyl),[12h] [(^{Ar}L)Co(NAd)] (1.424(8) Å; ^{Ar}L = 5-mesityl-1,9-(2,4,6-$Ph_3C_6H_2$)dipyrrin),[12k] and [(^{Tr}L)Co(NAd)] (1.431(5) Å; ^{Tr}L = 5-mesityl-1,9-(trityl)dipyrrin).[12l] Similarly, the linear Co–N(imido)–C(adamantyl) bond angle of 178.92(9)° is in line with other structurally characterized cobalt(III) imido complexes, and suggests the absence of a lone pair of electrons at the imido nitrogen atom.[12e–k] Thus, the short Co–N(imido) distance, together with the linear Co–N(imido)–C(adamantyl) bond, is indicative of multiple bonding within the Co–N(adamantyl) entity. As expected, the tertiary N-amine (N1) in pseudotetrahedral, divalent **1** and trigonal pyramidal, monovalent **2** is tetrahedral with average C-N–C bond angles of 114.3(3)° (**1**) and 113.5(1)° (**2**). In contrast, the corresponding N-anchor in trivalent **3** is trigonal planar, with C–N–C angles summing up to 357.8°. Furthermore, the average C–N(anchor) bond (1.433(3) Å) in trivalent **3** is significantly shortened compared with that in cobalt(I) complex **2** (1.464(2) Å). This observation is quite remarkable and suggests that N1 changes its hybridization from sp^3 in **2** to sp^2 in **3** upon oxidation and the introduction of the strongly bound AdN^{2-} imido ligand *trans* to N1. Accordingly, the structure of the literature-known and closely related Co^{III} imido TIMEN derivative [(TIMEN^{mes})Co(NAr^{OMe})]$^+$ was revisited in more detail (Figure S26 and Table S1), which revealed a similar unusual geometry with Σ(N-C-N) = 354.6°. Further literature research revealed that sp^2-hybridized tertiary amines are generally rare and, if observed, seldom discussed in the literature.[16] Furthermore, the the electronic origins of the planarization have not been discussed for the few transition-metal complexes with N-anchored, C_3-symmetric chelating ligands.[16] Just recently, Tomson and coworkers suggested that electrostatic interactions with the d(z^2)-orbital might be important for the metal–N(anchor) distance in copper(I) complexes.[17] Our computational analysis (see below) suggests that repulsive electrostatic interactions and negative hyperconjugation cause this structural feature.

Cyclic voltammetry studies of trivalent **3** in THF revealed a reversible oxidation process with $E_{1/2} = -0.30$ V versus $[FeCp_2]^0/[FeCp]^+$ (for details, see the Supporting Information). Accordingly, and in agreement with the electrochemical data, Co^{III} species **3** is readily oxidized by [$FeCp_2$](OTf) ($Cp^- = \eta^5$-$C_5H_5^-$; $OTf^- = CF_3SO_3^-$) in dichloromethane. However, all attempts to isolate the Co^{IV} complex at room temperature were complicated by the high reactivity of the target compound, as quantified by a half-life of less than 1 hour at 23 °C, according to UV/Vis electronic absorption spectroscopy. The UV/Vis spectrum of the oxidized product is distinct from that of **3**, with a broad band centered at λ_{max} = 583 nm ($\varepsilon = 1030\ M^{-1}cm^{-1}$; Figure S25). Although the product is thermally unstable, it is sufficiently stable at low temperatures to allow isolation and characterization. Accordingly, the dark green complex [(TIMMN^{mes})Co^{IV}(NAd)](OTf)$_2$ (**4**) could be synthesized in 94% yield from the precursor [(TIMMN^{mes})Co^{III}(NAd)](BPh_4) by the reaction of **3** with 2 equivalents of [$FeCp_2$](OTf) at −25 °C (Scheme 1). This is a one-electron oxidation accompanied by a BPh_4^-/TfO^- anion-exchange reaction.

Dark green crystals suitable for SC-XRD analysis were grown by slow diffusion of Et_2O into a THF solution of tetravalent **4** at −25 °C. The molecular structure of **4** in the solid state shows a pseudotetrahedral cobalt center that is supported by the TIMMN^{mes} chelator and the bound terminal imido ligand (Figure 1, **4**). The crystallographic data reveal that there are remarkably few structural changes upon oxidation of the cobalt(III) precursor **3** (Table 1). The one-electron oxidation Co^{III}→Co^{IV} is accompanied by a small but significant elongation of the Co–N(imido) bond from 1.649(1) Å in **3** to 1.702(3) Å in **4** and a slight shortening of the N(imido)–C(adamantyl) bond from 1.438(2) Å in **3** to 1.405(4) Å in **4**. Notably, the Co–N(imido) bond is also longer than the two equivalent Co=N bonds in the Co^{IV} bisimido complex [(IMes)Co(NDipp)$_2$][8] (1.665(3) Å). These findings contrast the results found with isoelectronic (and isostructural) Fe^{II}/Fe^{III} adamantyl imido groups supported by tris(phosphine)borate chelates.[18] In these complexes, the Fe–N(imido) bond shortens upon the oxidation of Fe^{II} (1.651(3) Å) to Fe^{III} (1.641(2) Å). In our cobalt complexes, oxidation results in the high-valent cobalt center moving deeper into the electron-rich cavity of TIMMN^{mes}, as is evident by the reduction of d_{oop}

Table 1: Summary of important structural parameters of trivalent **3** and tetravalent **4** in the solid state and as obtained by calculations at the TPSSh/ZORA-def2-SVP level of theory [in brackets].[a]

Parameter	3	4
d(Co=N8) [Å]	1.649(1) [1.636]	1.702(3) [1.748]
d(Co-N1) [Å]	3.374(2) [3.332]	2.659(3) [2.760]
d(C40-N8) [Å]	1.438(2) [1.426]	1.405(4) [1.401]
av d(Co-C) [Å]	1.936(1) [1.912]	2.004(2) [2.003]
d_{oop}(Co) [Å]	0.964(1) [0.937]	0.705(2) [0.723]
∡(Co-N8-C40) [°]	178.92(9) [179.5]	177.0(3) [179.7]
av ∡(C-Co-C) [°]	96.3(6) [97.8]	108.7(1) [107.7]
∡(N1-Co-N8) [°]	179.30(4) [179.7]	178.87(9) [179.6]
Σ(C-N-C) [°]	357.8 [358.8]	346.4 [351.9]

[a] A more complete table of metric parameters for complexes **1**–**4** and [(TIMEN^{mes})Co(NAr^{OMe})]$^+$ is given in the Supporting Information (Table S1). The value d_{oop} denotes the "out-of-plane" shift, which quantifies the distance at which the cobalt atom lies above or below the plane of the three carbene ligands.

(0.964(1) Å in **3**; 0.705(2) Å in **4**) and the significant shortening of the distance between the Co and the N1 atoms (3.374(2) Å in **3**; 2.659(3) Å in **4**). With respect to the above-mentioned sp^2-hybridized N1 in **3**, the amine anchor in **4** is sp^3-hybridized again, with Σ(C-N-C = 346.4°). More remarkable is the fact that the average Co–C bond length also significantly increases from 1.936(1) Å in the Co^{III} complex to 2.004(2) Å in the Co^{IV} complex. This difference may be due to enhanced π-backbonding in the case of **3**. This has also been observed for the isoelectronic (and isostructural) Fe^{II} and Fe^{III} adamantyl imido complexes supported by tris(phosphine)borate ligands,[18] where the one-electron oxidation of the Fe^{II} complex induced an elongation of the Fe–P bond by about 0.1 Å. The Co–N(imido)–C(adamantyl) bond angle of 177.0(3)° in **4** is similar to that found in its Co^{III} imido precursor **3** (178.92(9)°) and, thus, closer to linearity than in the Co^{IV} bisimido complex $[(IMes)Co(NDipp)_2]$[8] (173.0(3)°). This indicates that the one-electron oxidation does not greatly affect the Co–N(imido)–C(adamantyl) linkage.

In addition, the electronic structure of tetravalent **4** was studied by X-band EPR spectroscopy. The EPR spectrum of **4** (Figure 2), measured in THF at 7 K, displays a characteristic signal with the expected axial symmetry, centered at $g \approx 2$, and split into an eight-line pattern due to hyperfine coupling of the unpaired electron to the ^{59}Co nucleus ($I = 7/2$, 100% nat. abundance). No apparent super-hyperfine coupling of the nitrogen is observed. The best simulation to the experimental spectrum was obtained with an effective spin of $S = {}^1/_2$, and *g*-values at $g_\perp = 2.12$ and $g_\parallel = 2.09$, with hyperfine coupling constants of $A_\perp = 96.3 \times 10^{-4}\ cm^{-1}$ and $A_\parallel = 49.7 \times 10^{-4}\ cm^{-1}$. These data compare well to values reported for the Co^{IV} bisimido complex $[(IMes)Co(NDipp)_2]$ ($S = {}^1/_2$, $g_{av} \approx 1.98$)[8] and other Co^{IV} complexes ($g_{iso}/g_\parallel \approx 2.00$–$2.04$, $A_{iso(Co)}/A_{\parallel(Co)} =$ 20–30 G).[19] Thus, the EPR data for $[(TIMMN^{mes})Co(NAd)](OTf)_2$ (**4**) suggest a metal-centered oxidation of trivalent **3** and favor the formulation of complex **4** as a cobalt imido species with a metal oxidation state of + IV. Despite multiple attempts, and due to the pronounced thermal instability, reliable SQUID data could not be obtained for **4**.

A quantum chemical analysis was carried out to better understand the electronic structures of trivalent **3** and tetravalent **4**. Various density functionals (BP86, B97-3c, TPSSh, PBE0), including broken-symmetry calculations (Figure S34) and a wave-function method (CASSCF/NEVPT2) were evaluated. From the geometry-optimized molecular structures (Figure S35) and the modeled electronic absorption spectra using time-dependent DFT (TD-DFT; Figures S49–S55), we find that all methods give a consistent and appropriate description of the electronic structure of **3**. Importantly, the computational analysis (energy decomposition analysis of natural orbitals for chemical valence, EDA-NOCV; topological analysis of the Laplacian; noncovalent interaction NCI[20] plot) further corroborates the absence of a bonding orbital interaction between the amine anchor of the ligand and the cobalt ion and, instead, suggests a repulsive electrostatic interaction, which drives the planarization (Figures S63 and S64). Furthermore, these calculations indicate negative hyperconjugation with the adjacent methylene groups as well as minor interactions with the π-system of the NHC ligands (Figure 3, left; Figures S65–S67), which both

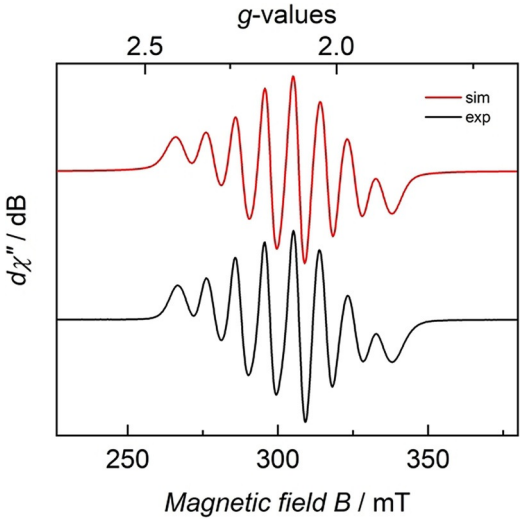

Figure 2. CW X-band EPR spectrum of $[(TIMMN^{mes})Co^{IV}(NAd)](OTf)_2$ (**4**), recorded as a 2 mM frozen THF solution at 7 K (black trace), and its simulation (red trace). Experimental conditions: microwave frequency $\nu = 8.959$ GHz, modulation width = 0.1 mT, microwave power = 1.0 mW, modulation frequency = 100 kHz, time constant = 0.1 s. Simulation parameters: effective spin $S = {}^1/_2$, effective *g*-values $g_\perp = 2.12$ and $g_\parallel = 2.09$, linewidths $W_\perp = 3.52$ mT and $W_\parallel = 7.46$ mT. Voigt ratios (Lorentz = 0, Gauss = 1) $V_\perp = 0.38$ $V_\parallel = 0.58$. Hyperfine coupling to one ^{59}Co ($I = 7/2$, 100% nat. abundance) nucleus was determined as $A_\perp = 96.3 \times 10^{-4}\ cm^{-1}$ and $A_\parallel = 49.7 \times 10^{-4}\ cm^{-1}$. A-strain effects were considered by using m_I-square-dependent linewidth broadening $c2 \cdot m_I^2$ with parameters $c2_\perp = 16.5 \times 10^{-4}\ cm^{-1}$ and $c2_\parallel = 3.48 \times 10^{-4}\ cm^{-1}$.

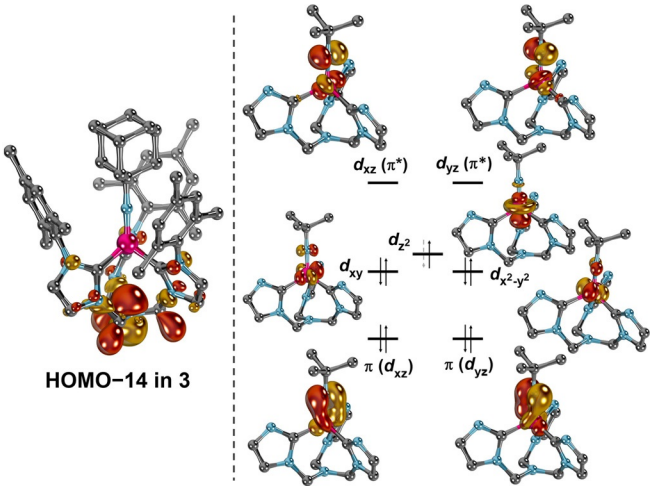

Figure 3. The lone pair of electrons at the sp^2-hybridized amine in **3** shows negative hyperconjugation with the adjacent methylene groups and does not mix with metal-centered orbitals (left; hydrogen atoms are omitted for clarity). The d-orbital splitting of the truncated cations of trivalent **3** (d^6) and tetravalent **4** (d^5) according to the lead configurations (**3**: 83%; **4**: 46%) in the CASSCF (10,7) and (9,7) calculations (right; orbitals of **4** are shown; mesityl and adamantyl groups as well as hydrogen atoms are omitted for clarity).

further stabilize the trigonal planar (e.g. TPSSh: Σ(C–N–C) = 358.8°) conformation of the amine.[21]

In contrast, the electronic structure of Co^{IV} species **4**, with its very covalent metal–ligand bonds, represents a challenge for common DFT methods, which show significant spin contamination. Whereas geometry optimizations of **4** with BP86 and B97-3c predict an insignificantly shorter (−0.01 Å) Co=NAd bond than for **3**, the hybrid functionals TPSSh (10% HF exchange) and especially PBE0 (25% HF exchange) predict a considerable elongation of the Co=NAd bond (TPSSh: +0.12 Å; PBE0: +0.22 Å) consistent with the experimental findings (+0.05 Å). Furthermore, the predictions of the *g*-values using TPSSh are in reasonable agreement with the EPR experiment (experiment: $g_\perp = 2.12$, $g_\parallel = 2.09$; BP86: $g_\perp = 2.09$, $g_\parallel = 2.07$; TPSSh: $g_\perp = 2.15$, $g_\parallel = 2.10$; PBE0: $g_\perp = 2.23$, $g_\parallel = 2.17$); the same is true for the hyperfine coupling constants (HFCs, Figures S43–S48). As the DFT methods struggled to reproduce the absorption spectrum of **4** (Figures S58–S62), we performed state-averaged NEVPT2/CASSCF calculations (Figures S56 and S57). Both DFT (Figure S42) and the CASSCF (Figure S68) calculations corroborate a d^6 electron configuration for the cobalt(III) complex **3**. Thereby, the molecular orbital, which relates to the $d(z^2)$-orbital, shows an admixture of s-character (18%), which likely reduces the antibonding interaction with the p(z)-orbital of the imido ligand as well as the repulsion with the electron lone pair of the nitrogen anchor of the ligand. Furthermore, the π-bonds between the imido ligand and the d(xz)- and d(yz)-orbitals of the cobalt ion are considerably covalent, with about 30% metal character.

Oxidation of **3** to **4** removes one electron from the $d(z^2)$-orbital, as is indicated by the weight of the lead configuration of 46% (Figure 3, right). This corroborates a formal oxidation state of +IV for the cobalt ion in **4** and suggests a reduced repulsive interaction with the N anchor of the ligand (cf. Figures S63–S68), thus, reducing the Co–N distance in analogy to the previously studied copper complexes[17] and attenuating the p(z)-character of the nitrogen atom's lone pair of electrons (e.g. TPSSh: **3**, Σ(C–N–C) = 358.8°; **4**, Σ(C–N–C) = 351.9°). Concomitantly, the covalency of the π-interaction between the metal's d(xz)- and d(yz)-orbitals with the imido ligand is further enhanced, with each having about 50% contribution. Accordingly, it is interesting to compare the Löwdin population analysis of Co^{IV} complex **4** by different methods. The CASSCF calculations indicate, in addition to the metal, accumulation of spin density also at the ligand (Co: +1.4 a.u.; N: −0.4 a.u.) and a bond order (BO) of only 1.3. This is due to partial excitation of 0.5 electrons each from the two π-symmetric orbitals between the imido ligand, p(x) and p(y), and the cobalt ion, d(yz) and d(xz), into the related π*-orbitals. The enhanced population of the antibonding π-orbitals in **4** (in comparison to **3**) is the electronic origin for the elongation of the Co–N bond length upon oxidation, as observed in the solid-state structure of **4** (Figure S70). Consequently, the density functionals (Figure S41) predict either a d^5 configuration (BP86: Co, +1.3 a.u.; N, −0.3 a.u., BO = 1.9) or a shift of electron density to the metal, thereby increasing the spin density at the ligand (TPSSh: Co, +1.8 a.u.; N, −0.8 a.u.; BO = 1.6; PBE0: Co, +2.1 a.u., N: −1.1 a.u., BO = 1.4). The latter picture emphasizes an antiferromagnetically coupled system, which relates either to an imidyl, that is, an imido-ligand-centered monoradical, or a triplet "nitrene", that is, an imido-ligand-centered diradical,[3] as illustrated by an analysis of the intrinsic bond orbitals[22] (Figure S42). Importantly, the minor configurations in the CASSCF calculations (Figures S37–S40) corroborate the DFT results and suggest in addition to the imido lead (46%) resonance structure, 30% nitrene and 18% imidyl character for the ground state of **4**. In concluding, the computational analysis indicates a d^5-configured cobalt(IV) ion with a very covalent double bond to the imido ligand, which shares partial nitrene as well as imidyl character.

Conclusion

In summary, a unique pair of Co^{III}/Co^{IV} imido complexes is presented. The rare high-valent cobalt(IV) monoimido complex $[(TIMMN^{mes})Co^{IV}(NAd)](OTf)_2$ (**4**) was synthesized by oxidation of its cobalt(III) imido precursor $[(TIMMN^{mes})Co^{III}(NAd)](BPh_4)$ (**3**). The molecular structure of the diamagnetic precursor **3** features an unusual sp^2-hybridized N atom in the chelate's amine anchor, which was computationally rationalized by negative hyperconjugation with the methylene groups of the pendant arms and repulsive electrostatic interaction with the metal center. EPR spectroscopy suggests a d^5 low-spin electron configuration at the central Co^{IV} ion in **4**, with the majority of the spin density residing at the metal center. Computational analyses corroborate the +IV oxidation state and advocate a cobalt–nitrogen double bond, but further suggest significant spin density at the imido ligand, which translates into significant nitrene character. Finally, it is interesting to note that oxidation of TIMEN-ligand-supported terminal Co^{III} imido and Fe^{IV} nitrido complexes results in insertion of the imide and nitride groups into the metal–carbene bonds, with the TIMMN ligand enabling isolation of the high-valent Co^{IV} and Fe^{V} complexes. The reactivity of **3** and **4** is currently under investigation.

Acknowledgements

This work was supported by funds of the German Federal Ministry of Education and Research (BMBF support code 03SF0502) and the FAU. W.M. acknowledges a research fellowship from the Alexander-von-Humboldt foundation. D.M. thanks the Fonds der Chemischen Industrie for a Liebig fellowship and the German-American Fulbright Commission for their support. Dr. Sadig Aghazada (FAU) is acknowledged for insightful discussions. We also thank Daniel Pividori (FAU) for collecting SQUID magnetization data, and the RRZE for computational resources. Open access funding enabled and organized by Projekt DEAL.

Conflict of interest

The authors declare no conflict of interest.

Keywords: cobalt · density functional theory calculations · EPR spectroscopy · N-heterocyclic carbenes · terminal imides

[1] a) P. Müller, C. Fruit, *Chem. Rev.* **2003**, *103*, 2905 – 2919; b) L. Zhang, L. Deng, *Chin. Sci. Bull.* **2012**, *57*, 2352 – 2360; c) K. Shin, H. Kim, S. Chang, *Acc. Chem. Res.* **2015**, *48*, 1040 – 1052; d) P. F. Kuijpers, J. I. van der Vlugt, S. Schneider, B. de Bruin, *Chem. Eur. J.* **2017**, *23*, 13819 – 13829; e) Y. Park, Y. Kim, S. Chang, *Chem. Rev.* **2017**, *117*, 9247 – 9301; f) Y. Liu, T. You, H. X. Wang, Z. Tang, C. Y. Zhou, C. M. Che, *Chem. Soc. Rev.* **2020**, *49*, 5310 – 5358; g) R. Eikey, *Coord. Chem. Rev.* **2003**, *243*, 83 – 124; h) J. F. Berry, *Comments Inorg. Chem.* **2009**, *30*, 28 – 66; i) C. T. Saouma, J. C. Peters, *Coord. Chem. Rev.* **2011**, *255*, 920 – 937; j) K. Ray, F. Heims, F. F. Pfaff, *Eur. J. Inorg. Chem.* **2013**, 3784 – 3807.

[2] F. Dielmann, D. M. Andrada, G. Frenking, G. Bertrand, *J. Am. Chem. Soc.* **2014**, *136*, 3800 – 3802.

[3] K. M. Carsch, I. M. DiMucci, D. A. Iovan, A. Li, S. Zheng, C. J. Titus, S. J. Lee, K. D. Irwin, D. Nordlund, K. M. Lancaster, T. A. Betley, *Science* **2019**, *365*, 1138 – 1143.

[4] a) E. R. King, E. T. Hennessy, T. A. Betley, *J. Am. Chem. Soc.* **2011**, *133*, 4917 – 4923; b) D. A. Iovan, T. A. Betley, *J. Am. Chem. Soc.* **2016**, *138*, 1983 – 1993; c) M. J. T. Wilding, D. A. Iovan, A. T. Wrobel, J. T. Lukens, S. N. MacMillan, K. M. Lancaster, T. A. Betley, *J. Am. Chem. Soc.* **2017**, *139*, 14757 – 14766.

[5] a) C. M. Thomas, N. P. Mankad, J. C. Peters, *J. Am. Chem. Soc.* **2006**, *128*, 4956 – 4957; b) E. J. Klinker, T. A. Jackson, M. P. Jensen, A. Stubna, G. Juhasz, E. L. Bominaar, E. Munck, L. Que, Jr., *Angew. Chem. Int. Ed.* **2006**, *45*, 7394 – 7397; *Angew. Chem.* **2006**, *118*, 7554 – 7557; c) I. Nieto, F. Ding, R. P. Bontchev, H. Wang, J. M. Smith, *J. Am. Chem. Soc.* **2008**, *130*, 2716 – 2717; d) K. Searles, S. Fortier, M. M. Khusniyarov, P. J. Carroll, J. Sutter, K. Meyer, D. J. Mindiola, K. G. Caulton, *Angew. Chem. Int. Ed.* **2014**, *53*, 14139 – 14143; *Angew. Chem.* **2014**, *126*, 14363 – 14367; e) H. Zhang, Z. Ouyang, Y. Liu, Q. Zhang, L. Wang, L. Deng, *Angew. Chem. Int. Ed.* **2014**, *53*, 8432 – 8436; *Angew. Chem.* **2014**, *126*, 8572 – 8576; f) L. Wang, L. Hu, H. Zhang, H. Chen, L. Deng, *J. Am. Chem. Soc.* **2015**, *137*, 14196 – 14207; g) B. P. Jacobs, P. T. Wolczanski, Q. Jiang, T. R. Cundari, S. N. MacMillan, *J. Am. Chem. Soc.* **2017**, *139*, 12145 – 12148; h) M. R. Anneser, G. R. Elpitiya, J. Townsend, E. J. Johnson, X. B. Powers, J. F. DeJesus, K. D. Vogiatzis, D. M. Jenkins, *Angew. Chem. Int. Ed.* **2019**, *58*, 8115 – 8118; *Angew. Chem.* **2019**, *131*, 8199 – 8202.

[6] a) C. Ni, J. C. Fettinger, G. J. Long, M. Brynda, P. P. Power, *Chem. Commun.* **2008**, 6045 – 6047; b) S. Hong, X. Lu, Y. M. Lee, M. S. Seo, T. Ohta, T. Ogura, M. Clemancey, P. Maldivi, J. M. Latour, R. Sarangi, W. Nam, *J. Am. Chem. Soc.* **2017**, *139*, 14372 – 14375; c) S. Hong, K. D. Sutherlin, A. K. Vardhaman, J. J. Yan, S. Park, Y. M. Lee, S. Jang, X. Lu, T. Ohta, T. Ogura, E. I. Solomon, W. Nam, *J. Am. Chem. Soc.* **2017**, *139*, 8800 – 8803.

[7] J. L. Martinez, S. A. Lutz, H. Yang, J. Xie, J. Telser, B. M. Hoffman, V. Carta, M. Pink, Y. Losovyj, J. M. Smith, *Science* **2020**, *370*, 356 – 359.

[8] L. Zhang, Y. Liu, L. Deng, *J. Am. Chem. Soc.* **2014**, *136*, 15525 – 15528.

[9] a) E. Kogut, H. L. Wiencko, L. Zhang, D. E. Cordeau, T. H. Warren, *J. Am. Chem. Soc.* **2005**, *127*, 11248 – 11249; b) V. M. Iluc, A. J. Miller, J. S. Anderson, M. J. Monreal, M. P. Mehn, G. L. Hillhouse, *J. Am. Chem. Soc.* **2011**, *133*, 13055 – 13063; c) S. Wiese, J. L. McAfee, D. R. Pahls, C. L. McMullin, T. R. Cundari, T. H. Warren, *J. Am. Chem. Soc.* **2012**, *134*, 10114 – 10121.

[10] a) Y. M. Badiei, A. Krishnaswamy, M. M. Melzer, T. H. Warren, *J. Am. Chem. Soc.* **2006**, *128*, 15056 – 15057; b) Y. M. Badiei, A. Dinescu, X. Dai, R. M. Palomino, F. W. Heinemann, T. R. Cundari, T. H. Warren, *Angew. Chem. Int. Ed.* **2008**, *47*, 9961 – 9964; *Angew. Chem.* **2008**, *120*, 10109 – 10112; c) M. J. Aguila, Y. M. Badiei, T. H. Warren, *J. Am. Chem. Soc.* **2013**, *135*, 9399 – 9406.

[11] a) J. Du, L. Wang, M. Xie, L. Deng, *Angew. Chem. Int. Ed.* **2015**, *54*, 12640 – 12644; *Angew. Chem.* **2015**, *127*, 12831 – 12835; b) Y. Liu, J. Du, L. Deng, *Inorg. Chem.* **2017**, *56*, 8278 – 8286; c) X. Yao, J. Du, Y. Zhang, X. Leng, M. Yang, S. Jiang, Z. Wang, Z. Ouyang, L. Deng, B. Wang, S. Gao, *J. Am. Chem. Soc.* **2017**, *139*, 373 – 380.

[12] a) D. M. Jenkins, T. A. Betley, J. C. Peters, *J. Am. Chem. Soc.* **2002**, *124*, 11238 – 11239; b) T. A. Betley, J. C. Peters, *J. Am. Chem. Soc.* **2003**, *125*, 10782 – 10783; c) X. Dai, P. Kapoor, T. H. Warren, *J. Am. Chem. Soc.* **2004**, *126*, 4798 – 4799; d) X. Hu, K. Meyer, *J. Am. Chem. Soc.* **2004**, *126*, 16322 – 16323; e) D. T. Shay, G. P. Yap, L. N. Zakharov, A. L. Rheingold, K. H. Theopold, *Angew. Chem. Int. Ed.* **2005**, *44*, 1508 – 1510; *Angew. Chem.* **2005**, *117*, 1532 – 1534; f) M. P. Mehn, S. D. Brown, D. M. Jenkins, J. C. Peters, J. L. Que, *Inorg. Chem.* **2006**, *45*, 7417 – 7427; g) R. E. Cowley, R. P. Bontchev, J. Sorrell, O. Sarracino, Y. Feng, H. Wang, J. M. Smith, *J. Am. Chem. Soc.* **2007**, *129*, 2424 – 2425; h) C. Jones, C. Schulten, R. P. Rose, A. Stasch, S. Aldridge, W. D. Woodul, K. S. Murray, B. Moubaraki, M. Brynda, G. La Macchia, L. Gagliardi, *Angew. Chem. Int. Ed.* **2009**, *48*, 7406 – 7410; *Angew. Chem.* **2009**, *121*, 7542 – 7546; i) E. R. King, G. T. Sazama, T. A. Betley, *J. Am. Chem. Soc.* **2012**, *134*, 17858 – 17861; j) B. Wu, R. Hernandez Sanchez, M. W. Bezpalko, B. M. Foxman, C. M. Thomas, *Inorg. Chem.* **2014**, *53*, 10021 – 10023; k) Y. Baek, T. A. Betley, *J. Am. Chem. Soc.* **2019**, *141*, 7797 – 7806; l) Y. Baek, E. T. Hennessy, T. A. Betley, *J. Am. Chem. Soc.* **2019**, *141*, 16944 – 16953; m) A. Reckziegel, C. Pietzonka, F. Kraus, C. G. Werncke, *Angew. Chem. Int. Ed.* **2020**, *59*, 8527 – 8531; *Angew. Chem.* **2020**, *132*, 8605 – 8609.

[13] M. Keilwerth, L. Grunwald, W. Mao, F. W. Heinemann, J. Sutter, E. Bill, K. Meyer, *J. Am. Chem. Soc.* **2021**, *143*, 1458 – 1465.

[14] X. Hu, I. Castro-Rodriguez, K. Meyer, *J. Am. Chem. Soc.* **2004**, *126*, 13464 – 13473.

[15] D. M. Jenkins, A. J. Di Bilio, M. J. Allen, T. A. Betley, J. C. Peters, *J. Am. Chem. Soc.* **2002**, *124*, 15336 – 15350.

[16] M. Yang, T. Albrecht-Schmitt, V. Cammarata, P. Livant, D. S. Makhanu, R. Sykora, W. Zhu, *J. Org. Chem.* **2009**, *74*, 2671 – 2678.

[17] A. B. Weberg, S. P. McCollom, L. M. Thierer, M. Gau, P. Carroll, N. C. Tomson, *Chem. Sci.* **2021**, *12*, 4395 – 4404.

[18] S. D. Brown, J. C. Peters, *J. Am. Chem. Soc.* **2005**, *127*, 1913 – 1923.

[19] a) J. Halpern, M. S. Chan, J. Hanson, T. S. Roche, J. A. Topich, *J. Am. Chem. Soc.* **1975**, *97*, 1606 – 1608; b) J. Halpern, J. Topich, K. I. Zamaraev, *Inorg. Chim. Acta* **1976**, *20*, L21 – L24; c) J. Topich, J. Halpern, *Inorg. Chem.* **1979**, *18*, 1339 – 1343; d) F. C. Anson, T. J. Collins, R. J. Coots, S. L. Gipson, T. G. Richmond, *J. Am. Chem. Soc.* **1984**, *106*, 5037 – 5038; e) M. Koikawa, M. Gotoh, H. Okawa, S. Kida, T. Kohzuma, *J. Chem. Soc. Dalton Trans.* **1989**, 1613 – 1616; f) G. B. Carpenter, G. S. Clark, A. L. Rieger, P. H. Rieger, D. A. Sweigart, *J. Chem. Soc. Dalton Trans.* **1994**, 2903 – 2910; g) P. H. Rieger, *Coord. Chem. Rev.* **1994**, *135/136*, 203 – 286; h) S. Will, J. Lex, E. Vogel, V. A. Adamian, E. V. Caemelbecke, K. M. Kadish, *Inorg. Chem.* **1996**, *35*, 5577 – 5583; i) E. M. Zolnhofer, M. Kaess, M. M. Khusniyarov, F. W. Heinemann, L. Maron, M. van Gastel, E. Bill, K. Meyer, *J. Am. Chem. Soc.* **2014**, *136*, 15072 – 15078; j) J. A. Bellow, S. A. Stoian, J. van Tol, A. Ozarowski, R. L. Lord, S. Groysman, *J. Am. Chem. Soc.* **2016**, *138*, 5531 – 5534.

[20] E. R. Johnson, S. Keinan, P. Mori-Sanchez, J. Contreras-Garcia, A. J. Cohen, W. Yang, *J. Am. Chem. Soc.* **2010**, *132*, 6498 – 6506.
[21] P. von R. Schleyer, A. J. Kos, *Tetrahedron* **1983**, *39*, 1141 – 1150.
[22] G. Knizia, *J. Chem. Theory Comput.* **2013**, *9*, 4834 – 4843.

Manuscript received: March 3, 2021
Revised manuscript received: March 29, 2021
Accepted manuscript online: April 13, 2021
Version of record online: June 18, 2021

